World Academy of Science, Engineering and Technology
International Journal of Geological and Environmental Engineering
Vol:9, No:8, 2015

Assessment of Agricultural Land Use Land Cover, Land Surface Temperature and Population Changes Using Remote Sensing and GIS: Southwest Part of Marmara Sea, Turkey

Melis Inalpulat, Levent Genc

***Abstract*—**Land Use Land Cover (LULC) changes due to human activities and natural causes have become a major environmental concern. Assessment of temporal remote sensing data provides information about LULC impacts on environment. Land Surface Temperature (LST) is one of the important components for modeling environmental changes in climatological, hydrological, and agricultural studies. In this study, LULC changes (September 7, 1984 and July 8, 2014) especially in agricultural lands together with population changes (1985-2014) and LST status were investigated using remotely sensed and census data in South Marmara Watershed, Turkey. LULC changes were determined using Landsat TM and Landsat OLI data acquired in 1984 and 2014 summers. Six-band TM and OLI images were classified using supervised classification method to prepare LULC map including five classes including Forest (F), Grazing Land (G), Agricultural Land (A), Water Surface (W), Residential Area-Bare Soil (R-B) classes. The LST image was also derived from thermal bands of the same dates.

LULC classification results showed that forest areas, agricultural lands, water surfaces and residential area-bare soils were increased as 65751 ha, 20163 ha, 1924 ha and 20462 ha respectively. In comparison, a dramatic decrement occurred in grazing land (107985 ha) within three decades. The population increased 29% between years 1984-2014 in whole study area. Along with the natural causes, migration also caused this increase since the study area has an important employment potential. LULC was transformed among the classes due to the expansion in residential, commercial and industrial areas as well as political decisions. In the study, results showed that agricultural lands around the settlement areas transformed to residential areas in 30 years.

The LST images showed that mean temperatures were ranged between 26-32°C in 1984 and 27-33°C in 2014. Minimum temperature of agricultural lands was increased 3°C and reached to 23°C. In contrast, maximum temperature of A class decreased to 41°C from 44°C. Considering temperatures of the 2014 R-B class and 1984 status of same areas, it was seen that mean, min and max temperatures increased by 2°C.

As a result, the dynamism of population, LULC and LST resulted in increasing mean and maximum surface temperatures, living spaces/industrial areas and agricultural lands.

***Keywords*—**Census data, landsat, land surface temperature (LST), land use land cover (LULC).

M. Inalpulat is with the Canakkale Onsekiz Mart University Faculty of Agriculture, Agricultural Sensor and Remote Sensing Lab. (ASRESEL) Canakkale, 17020 Turkey (corresponding author to provide phone: 0090-286-218-0018/1315; fax: 0090-286-218-0545; e-mail: melisinalpulat@gmail.com).

L. Genc, is with Canakkale Onsekiz Mart University Faculty of Agriculture, Agricultural Sensor and Remote Sensing Lab. (ASRESEL) Canakkale, 17020 Turkey (e-mail: leventgc@comu.edu.tr).

I. Introduction

SOCIO-ECONOMIC and political conditions determine status of a specific area as well as climatic conditions. However, the most important factor is the pressure resulted from population growth [1]. Along with the natural causes, migration from economically depressed rural areas to urban areas for a better living and job takes place as contributor to this growth. As a result, the demand for built up area is likely to increase as well [2]. Researches denoted that the rate of urbanization is twice the rate of urban population increase, and 30% of world population is expected to live in urban areas in near future [1]. On the other hand, it was reported that other land cover types such as; bare lands and vegetation may tend to decrease against increasing impermeable surfaces in further stages of such processes. Therefore, continuous changes in LULC status mostly appear in respect to human habitation, and the process called urbanization.

Since expansion in urban areas may affect not only the environment, inhabitants and biodiversity, but also the climate parameters especially temperature trends, it became essential to monitor LULC/LST changes for many environmental studies. The improvements in remote sensing satellites such as Landsat series which primarily launched in the beginnings of 1970s have provide a crucial tool for LULC researches. Furthermore, beside the visible and near/mid infrared sensitive bands, thermal bands of Landsat satellites serve as a high resolution source of emissivity studies. Landsat derived LST enabled researchers to estimate radiation budgets, heat balance, evapotranspiration and etc. The capability of Landsat imageries to develop LULC and surface temperature maps is well documented by several researchers [3], [4].

In this study, it was aimed to investigate the LULC and LST changes occurred especially in agricultural lands in response to population growth in Southwest part of Marmara Region of Turkey. The area was chosen due to its key role for agricultural production. A big percentage of agricultural products are exported to meet the demands of cosmopolitan cities such as Istanbul and Bursa.

II. Materials and Methods

A. Study Area

The study was conducted in South Marmara Watershed located at southwest part of Marmara Sea, Turkey. Study

covers approximately 490 thousand ha area, including 5 districts of Canakkale province (Canakkale Provincial Center, Biga, Can, Lapseki and Yenice districts) and Gonen district of Balikesir province. Fig. 1 illustrates the geographical location and the Landsat imagery coverage of study area.

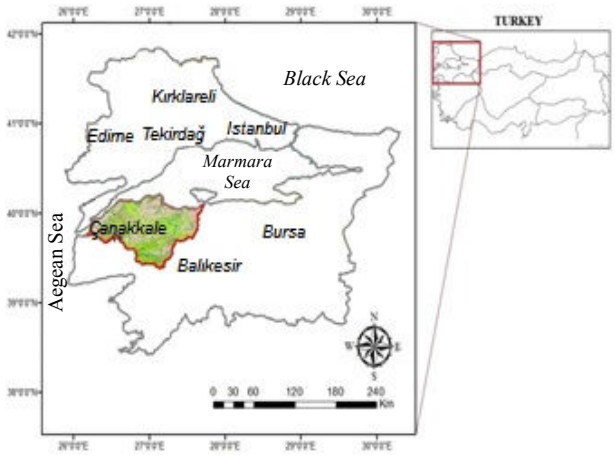

Fig. 1 The location of study area covered by Landsat OLI imagery

TABLE I
LANDSAT TM BANDS

Band No	Wavelength (μm)	Region
1	0.45-0.52	Visible
2	0.52-0.60	Visible
3	0.63-0.69	Visible
4	0.76-0.90	Near-Infrared
5	1.55-1.75	Mid-Infrared
7	2.08-2.35	Mid-Infrared

TABLE II
LANDSAT OLI BANDS

Band No	Wavelength (μm)	Region
2	0.45-0.51	Visible
3	0.53-0.59	Visible
4	0.64-0.67	Visible
5	0.85-0.88	Near-Infrared
6	1.57-1.65	Mid-Infrared
7	2.11-2.29	Mid-Infrared

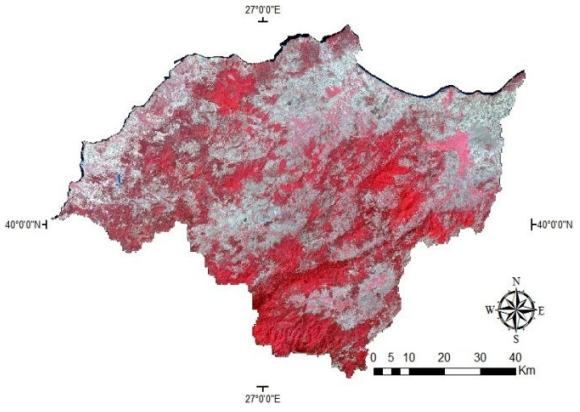

Fig. 2 Six-Band Landsat image of study area: 1984

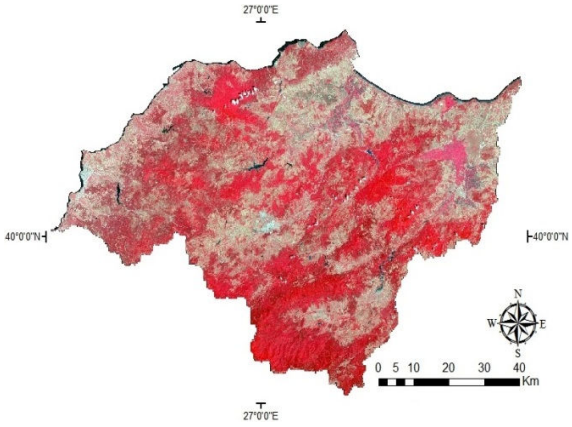

Fig. 3 Six-Band Landsat image of study area: 2014

B. LULC Map Development

Landsat satellite data with UTM projection have been downloaded from USGS. The Path/Row numbers of the concerning scene is 181/32. Landsat TM and OLI imageries relating to September 07, 1984 and July 08, 2014 were used to determine LULC status of each year. Six-band Landsat images were used to generate LULC maps of study area. Table I and II show the bands used in LULC classifications. In addition Figs. 2 and 3 show 6-band images for 1984 and 2014, respectively.

These six-band images have been used to obtain LULC maps by adopting maximum likelihood supervised classification algorithm (Erdas Imagine 2011 Software). Five main LULC classes were considered as; Forest (F), Grazing Lands (G), Agricultural Lands (A), Water Bodies (W) and Residential Area-Bare Soil (R-B). Forest class covered any kinds of forest trees. Grazing Lands included not only formal grazing lands and pastures, but also scrubs and moors. The study area has a mixed cropping pattern. However, agricultural lands were identified in particular without discrimination of any subgroups such as; orchards, irrigated crops, dry farming and etc. Water bodies involve dams, ponds and wetlands. The R-B class covered the built-up areas, roads, open mines, rocky areas and bare soils.

Accuracies of classifications were assessed referring field information (GPS points, photos and annotation records), visual interpretation, Google Earth, and Corona Images. In this step, accuracies of 150 randomized points were checked. These randomized points were taken automatically by software depending on area extents of classes and a minimum of 10 points per class were assessed in the study.

C. Population Change

Census data were downloaded from the website of Turkish Statistical Institute [5]. Since the census data was collected every five years (between 1965 and 2000), population data for 1984 was not available. Thus, the data belong to 1985 was used in the study. On the other hand, population census recorded annually after 2007.

Rural and urban populations of study area were considered in study. Census data of the six main settlements were obtained concerning urban and rural data, and the changes

between declared years were investigated.

In addition, the relationships between urban expansion and population were evaluated using regression analysis (Minitab 16). The LULC maps of provinces were subtracted from LULC map of whole study area using official province boundaries in ArcGIS 10.3 (ESRI, Redlands CA, USA) software. The change occurred within province boundaries were assessed together with related population data.

D. Land Surface Temperature (LST)

Land Surface Temperature (LST) for each pixel was computed from thermal bands of the Landsat images of given dates (Erdas Imagine 2011). The LST computation includes several steps including Converting digital numbers (DN) to spectral radiance (L), Converting spectral radiance to Kelvin temperature (T_B °K), Conversion of Kelvin temperature to Celsius using (1)-(3) [6]-[13]:

$$L = L_{min} + (L_{max} - L_{min}) \times \left(\frac{DN}{2^n - 1}\right) \quad (1)$$

$$T_B\,(°K) = \frac{K_2}{\ln\left(\frac{K_1}{L} + 1\right)} \quad (2)$$

$$T_B(°C) = T_B(°K) - 273 \quad (3)$$

where; *Lmin*: Spectral radiance of DN value 1; *Lmax*: Spectral radiance of DN value (2^n-1); *n*: Radiometric resolution of image; K_1: Calibration constant 1; K_2: Calibration constant 2; T_B: Surface temperature.

Table III shows the spectral radiance, n and calibration constant values used in the study. These values can be found in header file of specific Landsat download.

TABLE III
PROPERTIES OF LANDSAT TM/TIRS THERMAL BANDS

Properties	Landsat TM (Band 6)	Landsat TIRS (Band 10)	Landsat TIRS (Band 11)
Band Range (μm)	10.40-12.50	10.60-11.19	11.50-12.51
L_{min}	1.23800	1.10033	1.10033
L_{max}	15.30300	22.00180	22.00180
n	8	16	16
K_1	607.76	774.89	480.89
K_2	1260.56	1321.08	1201.14

Finally, descriptive statistics of LST for each LULC classes were calculated using ArcGIS Software 10.3.

III. RESULTS AND DISCUSSIONS

A. LULC Classification Results

The results of LULC classification indicated that forest and grazing land were the dominant LULC classes in 1984 with areas of 230274 ha and 229864 ha, respectively. Agricultural lands had an area of 164602 ha while area of R-B class found to be approximately 12400 ha. Area of water surfaces was 3568 ha. Fig. 4 represents LULC map of 1984.

Considering 2014 LULC map, it was seen that F class (319373 ha) was the dominant class and followed by A class (172452 ha), G class (116901 ha), R-B class (26968 ha), and W class (5015 ha) (Fig. 5). The areas for each LULC class and alternations between years are given in Table IV as percentages.

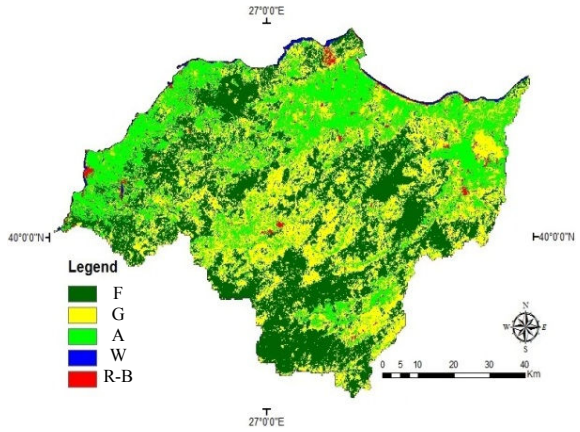

Fig. 4 LULC map regarding 1984 derived from 6-band Landsat TM

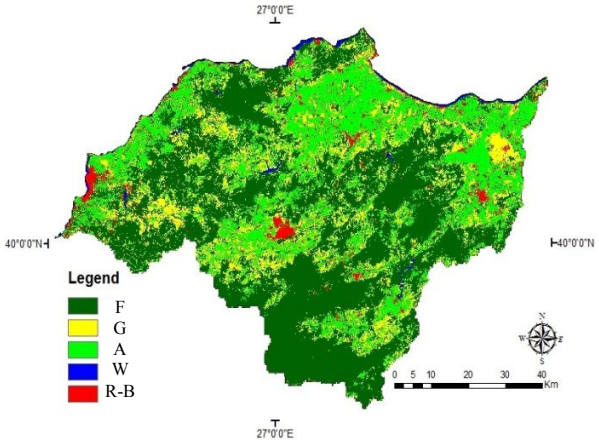

Fig. 5 LULC map regarding 2014 derived from 6-band Landsat OLI

TABLE IV
CHANGES IN LULC CLASSES BETWEEN 1984 AND 2014

LULC Class	Proportions of LULC Classes (%)			
	1984	2014	Change	
F	35.94	49.85	13.91	+
G	35.88	18.25	17.63	-
A	25.69	26.91	1.22	+
W	0.55	0.78	0.23	+
R-B	1.94	4.21	2.27	+
Total	100	100	35.26	

The area of forest class seemed to increase from 230274 ha to 319373 ha which is equivalent to 13.91%. It is believed that this increment is not only caused by the actual change in forests, but also resulted from the spectral similarity of reforestation areas and grazing lands in 1984. Since the spectral responses of reforestation areas may be similar to grazing land class, reforestation areas could be classified in G class. However, since alternation occurred in spectral properties of these young trees in time, they appeared to be classified in F class in 2014. On the other hand, this approach also explains the remarkable decrease in grazing lands. A

slight increase of 7850 ha occurred in A class (1.22%). Constructions of new dams and ponds in study area lead to increment in W class (1447 ha, and 0.23 in percentage). As a result, the overall change was found to be 35.26%. Kappa statistics and accuracies are 0.8261 and 88.60% for 2014, and 0.7296 and 78.20% for 1984 years.

A considerable part of agricultural lands around the settlements found to be transformed into R-B class within three decades. This tendency caused from rapid expansion in urban areas due to growing population. However, transforming of G class into A class provided maintenance of total amount of agricultural lands. In Fig. 6, A represents R-B class subtraction of 2014 LULC map, and B represents the past LULC status of these areas. In addition, the magnitudes of transformations (%) from each LULC to R-B class are given in Table V. It was seen that 61.69% proportion of residential areas were gained from agricultural lands while only 22. 52% were included in R-B class in the past.

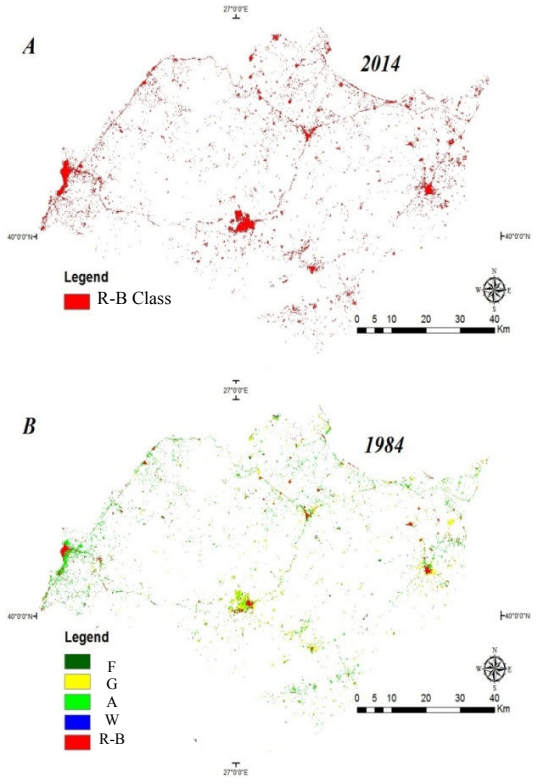

Fig. 6 A. R-B class subtracted from 2014 LULC map, B. The LULC status of same area in 1984

TABLE V
TRANSFORM OF LULC CLASSES TO R-B CLASS

LULC Class	Transform Proportions of LULC Classes (%) 2014 R-B
1984 F	5.94
1984 G	9.67
1984 A	61.69
1984 W	0.18
1984 R-B	22.52
Total	100

B. Relations between Population and LULC

Census data showed that a great majority of the population (79%) was living in rural areas in 1965. However, rural population presented a decrease within years and declined to 40%. Conversely, urban population reached to 60% which was only 21% at the beginning. Finally, the overall population of study area was 270290 in 1965 while it is reported as 424466 currently. The temporal changes in rural, urban and overall (total) population can be seen on Fig. 7. The increase was found to be 29% for overall population.

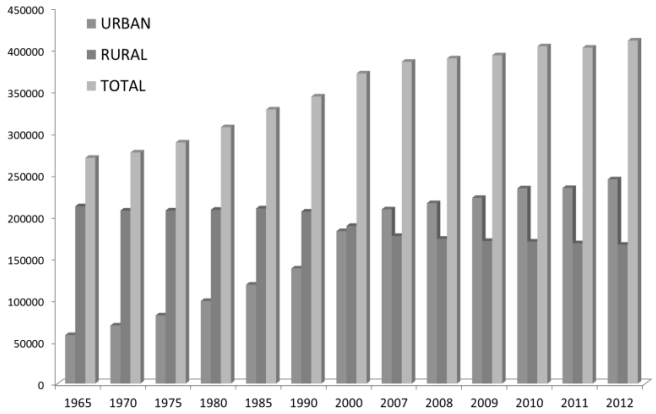

Fig. 7 Temporal changes of cencus data records depending on rural, urban and overall populations

Main reason for expansion in urban areas which are classified in R-B class seemed to arise from increase trend of populations. The result of regression analysis between census data and urban areas within extracted LULC maps supported this assumption. Regression analysis was conducted using populations against each related provinces. Fig. 8 illustrates regression between population and R-B class. Nevertheless, construction of thermal power plant in Can district, operations on open mines, and enlargements in similar work industries may be cited as a secondary reason of increased value of R-B class.

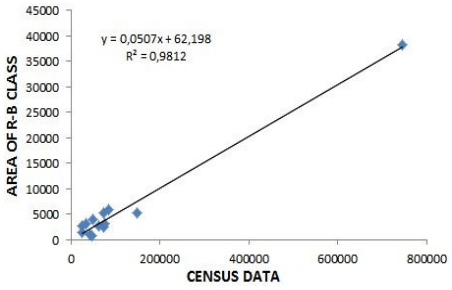

Fig. 8 Regression between population and area (ha) of R-B class

C. LST Interpretation for LULC Classes

Figs. 9 and 10 represent LST maps derived from 1984 and 2014 imageries respectively. Since the Landsat 8 (TIRS) has two bands in thermal infrared region of electromagnetic spectrum, LST was calculated averaging two individual LST images obtained from relating two bands.

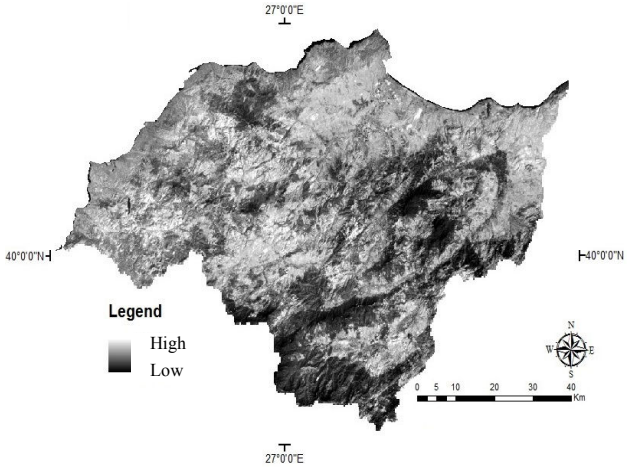

Fig. 9 Instantaneous LST status of study area in 1984

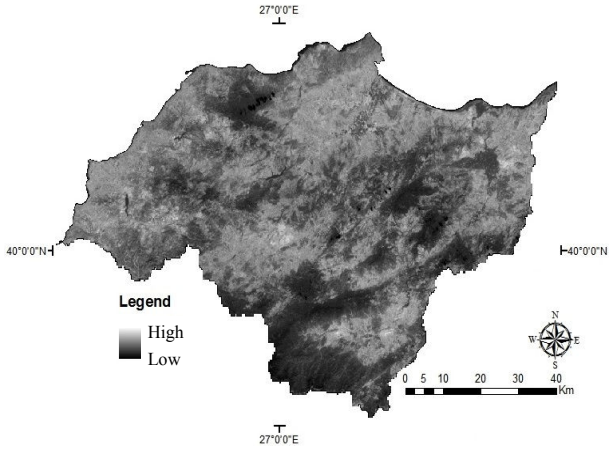

Fig. 10 Instantaneous LST status of study area in 2014

Statistics for LST including minimum temperatures (°C), maximum temperatures (°C), mean temperatures (°C), alternation ranges (°C), and standard deviations relating to each classes except W class. Water surfaces were not included in statistics since these kind of surfaces have cooler temperature in comparison with surroundings due to their thermal characteristics. Results are given in Tables VI and VII.

TABLE VI
TEMPERATURE (°C) STATISTICS OF LULC CLASSES: 1984 (BAND 6)

LULC	MIN	MAX	RANGE	MEAN	STD
F	18	38	20	26	3
G	18	43	25	31	3
A	20	44	24	32	3
R-B	19	44	25	32	3

TABLE VII
TEMPERATURE (°C) STATISTICS OF LULC CLASSES: 2014
(AVERAGE OF BAND 10 & BAND 11)

LULC	MIN	MAX	RANGE	MEAN	STD
F	21	38	17	27	2
G	24	42	18	32	2
A	23	41	18	32	2
R-B	21	42	21	33	2

Considering LST of whole study area, it was observed that min, and mean temperatures were increased while max temperatures were decreased. However, the decrease in max temperatures was low comparing to increase in min temperatures. Increased surface area of W class together with the increase in irrigated areas may have cooling effect on their surroundings. Unlikely to this impact, urban expansion is cited as the reason for increased temperatures. As evidence, the LST changes of the areas that transformed to urban (R-B class) were also investigated. The results showed that min, max and mean temperatures were found to be increased (Table VIII). However, since LST defined as the temperature emitted by surface, consideration of climatic parameters measured by meteorological stations together with LST would give more accurate results.

TABLE VIII
TEMPERATURE (°C) STATISTICS OF SUBTRACTED AREAS:
2014 R-B AREA AND 1984 STATUS OF SAME AREA

YEAR	MIN	MAX	RANGE	MEAN	STD
1984	19	40	21	31	2
2014	21	42	21	33	2

IV. CONCLUSION

Landsat TM and OLI-TIRS datasets were used to determine LULC and LST status for summer seasons of 1985 and 2014 years. A small increase of 1.22% was observed in magnitude of agricultural lands. However, expansion of urban areas was found to be 2.27%. It was seen that, almost 62% of A class located around residential areas were transformed into R-B class in this expansion process. These results were coherent with population growth indications. Considering LST, it was seen that minimum temperature of A class was increased, and maximum temperature was decreased while change observed for the mean temperature. On the other hand, LST of R-B-transformed areas increased 2°C (±2°C) for minimum, maximum and mean temperatures. In conclusion, due to the fact that LST offers results for instantaneous conditions, using long-years temperature data recorded by meteorological stations may provide better understanding of long term temperature trends.

REFERENCES

[1] M. S. Hassan, and S. Mahmud-ul-islam, "Urban area change Analysis in the Rangpur Sadar Upazila, Bangladesh using Landsat imageries", *International Journal of Science and Research*, vol. 4, no. 1, pp. 469-474, 2015.

[2] K. M. Kafi, H. Z. M. Shafri, and A. B. M. Shariff, "An analysis of lulc change detection using remotely sensed data; a case study of Bauchi city", *7th International Remote Sensing and GIS Conference and Exhibition Earth and Environmental Science*, vol. 20, pp. 1-9, 2014.

[3] K. Seto, C. E. Woodcock, C. Song, X. Huang, J. Lu, and, R. K. Kaufmann, "Monitoring land-use change in the Pearl River Delta using Landsat TM", *International Journal of Remote Sensing*, vol. 23, no. 10, 1985-2004, 2002.

[4] K. S. Kumar, P. U. Bhaskar, and K. Padmakumari, "Estimation of land surface temperature to study urban heat islamd effect using Landsat ETM+ image", *International Journal Engineering Science and Technology*, vol. 4, no. 2, pp. 771-778, 2012.

[5] TUIK, Turkish Statistical Institute, 2015 http://tuik.gov.tr.

[6] G. Chander, B. L. Markham, and D. L. Helder, "Summary of current radiometric calibration coefficients for Landsat MSS, TM, ETM+ and

EO-1 ALI sensors", *Remote Sensing of Environment*, vol. 113, no. 5, pp. 893-903, 2009.

[7] A. Fornaciai, M. Bisson, F. Mazzarini, P. D. Carlo, G. Pasquare, "Landsat 5 TM images and DEM in lithologic mapping of Payen Volcanic Field (Mendonazo Province, Argentina)", *Rivista Italiano Di Telerilevamento*, vol. 41, no. 1, pp. 11-24.

[8] C. Coll, J. M. Galve, J. M. Sanches, and V. Caselles, "Validation of Landsat-7/ETM+ thermal-band calibration and atmospheric correction with ground-based measurements", *IEEE Transactions on Geoscience and Remote Sensing*, vol. 48, no. 1, pp. 547-555, 2010.

[9] YCEO, Yale University Center for Earth Observation, http://www.yale.edu/ceo/Documentation/Landsat_DN_to_Kelvin.pdf

[10] NASA, National Aeronautics and Space Administration, 2011. http://landsathandbook.gsfc.nasa.gov/data_prod/prog_sect11_3.

[11] E. Tarantino, "Monitoring spatial and temporal distribution of sea surface temperature with TIR sensor data", *Italian Journal of Remote Sensing,* vol. 44, no. 1, pp. 97-107, 2012.

[12] E. Ozelkan, S. Bagis, E. C. Ozelkan, B. B. Ustundag, and C. Ormeci, "Land surface temperature retrieval for climate analysis and association with climate data", *European Journal of Remote Sensing*, vol. 47, pp. 655-669, 2014.

[13] O. Orhan, S. Ekercin, and F. Dadaser-Celik, "Use of Landsat land surface temperature and vegetation indices for monitoring drought in the salt lake basin area, Turkey", *Scientific World Journal*, vol. 2014, pp. 1-11, 2014.